

A NUMERICAL SIMULATION FOR EFFICIENCY ENHANCEMENT OF CZTS BASED THIN FILM SOLAR CELL USING SCAPS-1D[†]

 Muhammad Amir Shafi^{a,e,f,*}, Sumayya Bibi^b, Muhammad Muneeb Khan^c, Haroon Sikandar^d, Faisal Javed^c,  Hanif Ullah^e,  Laiq Khan^a,  Bernabe Mari^f

^aDepartment of Electrical and Computer Engineering, COMSATS University Islamabad, Pakistan

^bDepartment of Electrical Engineering, Bahauddin Zakariya University Multan, Pakistan

^cDepartment of Electrical Engineering, Pakistan Institute of Southern Punjab Multan, Pakistan

^dCEME, College of Electrical and Mechanical engineering, Nust Islamabad, Pakistan

^eDepartment of Electrical Engineering, Federal Urdu University of Arts Science and Technology, Islamabad, Pakistan

^fInstituto de diseño y Fabricación (IDF), Universitat Politècnica de València (UPV), Spain

*Corresponding Author: aamirshafi@ymail.com

Received March 28, 2022; revised April 3, 2022; accepted April 5, 2022

In this paper we proposed a solar cell having model “Back Contact/CZTS/ZnCdS/ZnO/Front Contact”. CZTS is working as an absorber layer, ZnCdS as a buffer layer and ZnO as a window layer with back and front contacts. The Zn content was varied from 0% to 10% and band gap was changed from 2.42 to 2.90 eV as described in the literature. The impact of this band gap variation has been observed on the performance of solar cell by using SCAPS-1D software. The efficiency was varied due to variation in bandgap of ZnCdS thin film layer. The simulation was carried out at 300 K under A.M. 1.5 G 1 Sun illumination. The energy bandgap diagram has been taken from SCAPS to explain the different parameters of solar cell. The effect of ZnCdS having different bandgap values was observed. Then the thickness of CZTS layer was varied to check its effect and hence at 3.0 μm gave the improved efficiency of 13.83% roundabout. After optimization of CZTS layer thickness, the effect of working temperature was examined on the performance of solar cell. The absorption coefficient variation from $1 \cdot 10^4$ to $1 \cdot 10^9 \text{ cm}^{-1}$ caused major effects on the characteristics parameters of solar cell along with on J-V characteristics and Quantum Efficiency curve. At $1 \cdot 10^9 \text{ cm}^{-1}$ absorption coefficient the efficiency of solar cell boost up to 16.24%. This is the remarkable improvement in the efficiency of solar cell from 13.82% to 16.24%. After optimization of all parameters, simulation was run at 280 K, having CZTS thickness of 3.5 μm , with 10% content Zn in ZnCdS (2.90 eV), and absorption coefficient of $1 \cdot 10^9$, the model efficiency reached up to 17.6% with Voc of 0.994 V, Jsc 26.1 mA/cm² and Fill factor was 71.4%.

Keywords: ZnCdS; CZTS; Simulation; Efficiency; SCAPS-1D

PACS: 02.60.Cb, 02.60.Pn, 82.47.Jk, 84.60.Jt, 42.79.Ek, 89.30.Cc

INTRODUCTION

Group II-VI semiconducting material of “Cadmium” focussed chalcogenide family have more modulation by academic researchers because of its excellent properties and potential contributions to the field of electrical, optoelectronic devices, light emitting, etc. Cadmium sulphide (CdS) is a chemical that belongs to the group II-VI. Cadmium telluride (CdTe), copper indium diselenide/sulphide (CIDS), and copper indium gallium diselenide/Sulphide (CIGS) solar cells are semiconductor materials that have uses in a variety of heterojunction photovoltaic systems [1]. CdS thin films exhibit significant attenuation due to their optoelectronic characteristics [2]. A study of the processing of certain III-V and II-VI binary compound semiconductors for technological applications was conducted [3,4,5]. The optical band-gap of CdS nanoparticles produced using the mw aided technique was investigated larger than that of bulk CdS nanoparticles [6,7]. The small bandgap reduces the power conversion efficiency by partially blocking transmission of high-energy photons to an absorber layer below. The larger bandgap of ZnxCd1-xS results in greater quantum efficiency in the blue part of the spectrum when CdS is substituted. The addition of Zn to the CdS buffer layer material lowers the lattice constant, resulting in a more advantageous conduction band alignment with a lattice match to the CIGS absorber. It has been discovered that adding Zn to CIGS solar cells improves both Voc and Jsc of solar cell, resulting in a better conversion efficiency [8,9]. ZnCdS may also be used to make p-n junctions with no lattice mismatch in quaternary materials like CuIn_xGa_{1-x}Se₂ or CuIn_xGa_{1-x}Se₂(S_xSe_{1-x})₂. By adjusting the Zn content, the growth characteristics of ZnCdS films may be fine-tuned. Different Zn concentrations control the pace of CdS development and are a key element in influencing the film's characteristics [10]. Ternary zinc cadmium sulfide (ZnCdS) has long been recognized as a suitable material for thin-film photovoltaic applications due to its high optical absorption coefficient [11]. Thin film Electrodeposition, chemical coprecipitation, spray pyrolysis, chemical vapor deposition, chemical bath deposition, and dip coating have all been used to make ZnCdS. Chemical bath deposition is one of the most used methods because of its convenience, simplicity, uniformity, stability, adhesion, homogeneity, and compactness with no pin holes thin films [12]. To improve the collection of short wavelength photons, minimize electron-hole recombination, as well as promote charge transfer to photoelectrode, ZnCdS was used as a window layer, and high efficiency has been achieved in thin copper indium gallium selenide (CIGSe₂) and copper indium gallium sulfide (CIGS₂) absorber layers [13,14]. A catalyst with a direct bandgap of 2.4 eV

[†] Cite as: M.A. Shafi, S. Bibi, M.M. Khan, H. Sikandar, F. Javed, H. Ullah, L. Khan, and B. Mari, East Eur. J. Phys. 2, 52 (2022), <https://doi.org/10.26565/2312-4334-2022-2-06>

© M.A. Shafi, S. Bibi, M.M. Khan, H. Sikandar, F. Javed, H. Ullah, L. Khan, B. Mari, 2022

for CdS and 3.7 eV for ZnS is thought to be effective [15]. ZnCdS has reasonable and adjustable absorbance based on the Zn/Cd ratio in the visible solar spectrum and good electrical conductivity [16,17]. As a result, ZnCdS is widely regarded as a competent bandgap material for photocatalytic degradation [18]. When Zn is doped with CdS to produce ZnCdS, the CdS bandgap increases to 3.7 eV due to the doped ZnS semiconductor bandgap. Because of this property, ZnCdS has been identified as an alternate buffer and window layer for solar cells, replacing CdS [19]. When Zn was doped with CdS, the material's resistance was found to be greater than that of CdS. In addition, Zn aids in the reduction of absorption losses at the window layer in CdS. The open circuit voltage and short circuit current in the hetero-junction structure grow as a result of this [20,21]. Because ZnCdS has a higher spectrum response than CdS due to the Zn component. The performance of ZnCdS-based solar devices will be greatly anticipated as a result of this characteristic, and ZnCdS will be employed as a suitable material for manufacturing p-n junctions. By raising the Zn content in the bath, the crystal size of ZnCdS was decreased. Furthermore, the absorption wavelength of CdS-based materials has been shown to change to lower wavelengths owing to Zn doping [22]. The effect of Zn on the CdS brings the changes in bandgap of ZnCdS according to the concentration of Zn, hence at each concentration the performance of Solar Cell is analyzed using SCAPS-1D Simulator.

SOLAR CELL MODEL AND NUMERICAL PARAMETERS

The solar model that has been used for the simulation in this research paper is shown in Figure. 1.

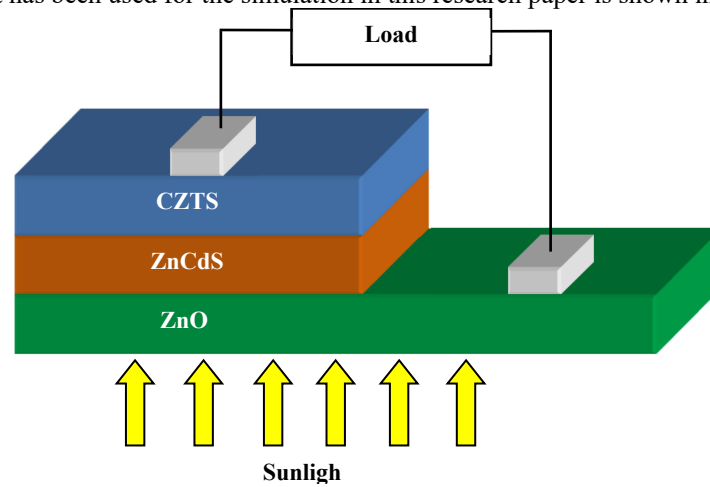


Figure 1. Solar cell model in Simulation.

To analyze the performance of the solar cell a one-dimensional software SCAPS-1D is used. The solar model that has been examined is consisting of CZTS absorber layer, ZnCdS is used as a buffer layer and ZnO is being used as window layer. Solar cell characteristics utilized in our simulation were chosen from academic literature, theories, and experiment-based results as shown in Table 1 [23]. The lighting spectrum is adjusted to AM1.5 G 1 sun, whereas working temperature is set to 300 K [24,25]. Quaternary semiconductors are difficult to manufacture and need a variety of time-consuming and costly technical processes. However, utilizing experimental techniques to confirm theoretical assumptions that are necessary in research is unavoidable [26]. Computer based simulation software allows time and money to be saved. It's a strong approach for predicting and assessing the influence of numerous model parameters and material characteristics on output performance of a solar cell. In this study, we use SCAPS software developed by Marc Bergeman and colleagues at the University of Gent [27,28].

When modelling solar cells, ensure that the program can solve the Poisson's equations for the charge electrostatic potential $div(\epsilon \nabla \Psi) = -\rho$ [29], as well as the carrier continuity equations for electrons and holes equations 1 and 2 [30].

$$\frac{\partial n}{\partial t} = \frac{1}{q} div \vec{J}_n + G_n - R_n, \quad (1)$$

$$\frac{\partial p}{\partial t} = -\frac{1}{q} div \vec{J}_p + G_p - R_p, \quad (2)$$

where,

n = concentration of electrons, p = concentration of holes, J_n = Electron current density, J_p = Hole current density, G_n = Electron Generation Rate, G_p = Hole Generation Rate, R_n = Electron Recombination Rate, R_p = Hole Recombination Rate

The influence of Zn content on ZnCdS layer plays an important role in varying its bandgap and hence this varied bandgap has been examined with CZTS based solar cell. After that the effect of CZTS thickness and absorption coefficient variation has been examined as well as effect of different temperatures on the performance of solar cell was next simulated.

The solar cell parameters used in simulation are listed below in Table 1. Whereas, parameters for both front and back contacts are shown in the Table 2.

Table 1. Numerical Parameters used for simulation [31,32].

Parameters	CZTS	ZnCdS	ZnO
$W (\mu m)$	2.00	0.10	0.05
$E_g (eV)$	1.55	2.42	3.35
$\chi (eV)$	4.500	4.440	4.210
ϵ_r	10.000	9.300	9.000
$N_C (cm^{-3})$	2.200E+18	2.100E+18	2.200E+18
$N_V (cm^{-3})$	1.800E+19	1.700E+19	1.800E+19
$V_e (cm/s)$	1.000E+7	1.000E+7	1.000E+7
$V_p (cm/s)$	1.000E+7	1.000E+7	1.000E+7
$\mu_e (cm^2/(Vs))$	1.000E+2	9.500E+1	2.500E+1
$\mu_p (cm^2/(Vs))$	2.000E+1	3.500E+1	1.000E+2
$N_D (cm^{-3})$	0.000E+0	2.500E+16	1.000E+18
$N_A (cm^{-3})$	8.220E+18	0.000E+0	0.000E+0
α	Scaps Value	Scaps Value	Scaps Value

Table 2. Simulation Parameters used for back and front contact from SCAP-1D.

Parameters	Front Contact	Back Contact
Surface recombination velocity of electrons (cm/s)	1.00×10^7	1.00×10^5
Surface recombination velocity of holes (cm/s)	1.00×10^5	1.00×10^7
Metal work function (eV)	4.6039	5.8973
Majority carrier barrier height relative to E_f (eV)	0.0539	0.1527
Majority carrier barrier height relative to E_v (eV)	0.0000	0.0000

Study as a function of Zn content in ZnCdS buffer layer

Both CdS and ZnCdS are semiconductors with a direct bandgap. Optical bandgap of semiconductors may then be calculated through graphing a square of the photon energy $(\alpha h\nu)^2$ vs photon energy ($h\nu$). A value of optical bandgap is determined through extrapolating a linear component of this curve to an energy axis. Figure 2 illustrates a curve of $(\alpha h\nu)^2$ as a function of photon energy for varied Zn concentrations in ZnCdS thin films. The results demonstrate that when the Zn concentration increases, the bandgap moves to higher energies. Table 3 shows the results for optical bandgaps ranging from 2.42 eV for CdS to 2.90 eV for various ZnCdS thin films. Figure 2 and Table 3 are taken from the article [33].

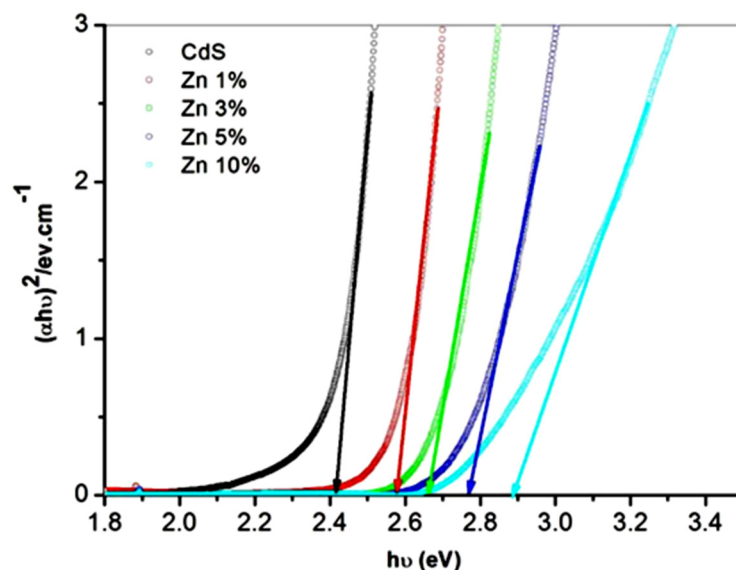


Figure 2. Plot of $(\alpha h\nu)^2$ vs photon energy ($h\nu$) for ZnCdS thin films with different Zn concentrations

Table 3. Optical bandgap for ZnCdS thin films with different Zn amounts

Sr#	Zn Content	ZnCdS band gap
	%	eV
1	0	2.42
2	1	2.58
3	3	2.67
4	5	2.78
5	10	2.90

To observe this varying bandgap effect on performance of CZTS based solar cell of proposed model “Glass/Back Contact/CZTS/ZnCdS/ZnO/Front Contact” has been simulated where the thickness of CZTS and ZnO was kept 2 μm and 0.05 μm respectively. The working temperature has been kept constant 300K. Series resistance is taken as to zero ohm where as the shunt resistance as infinite.

Study as a function of CZTS absorber layer thickness

To observe an effect of thickness of CZTS absorber layer in solar device model “Glass/Back Contact/CZTS/ZnCdS/ZnO/Front Contact” on performance of solar cell, thickness of ZnO layer was kept 0.05 μm and ZnCdS layer with thickness of 0.01 μm was used. The working temperature is maintained 300 K [34]. Series resistance is taken as to be zero ohm where as the shunt resistance as an infinite. The effect of CZTS thickness varying from 1.0 μm to 3.0 μm was simulated.

Study as a function of working temperature

To observe an effect of different working temperautes of solar cell model “Glass/Back Contact/CZTS/ZnCdS/ZnO/Front Contact” on a performance of solar cell, thickness of ZnO layer was kept 0.05 μm and ZnCdS layer with thickness of 0.01 μm was used. Whereas the thickness of CZTS absorber layer fixed was 2.0 μm . The series resistance is taken as to be zero ohm whereas the shunt resistance as an infinite. The effect of working temperature varying from 280 K to 350 K was simulated.

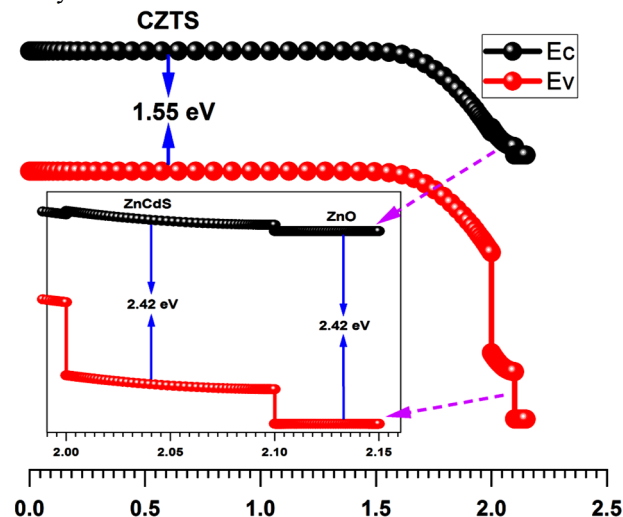
Study as a function of absorption coefficient

To observe an effect of absorption coefficient of absorber layer in solar cell model “Glass/Back Contact/CZTS/ZnCdS/ZnO/Front Contact” on performance of solar cell, thickness of ZnO layer was kept 0.05 μm and ZnCdS layer with thickness of 0.01 μm was used. Whereas the thickness of CZTS absorber layer fixed was 2.0 μm . The series resistance is taken as to be zero ohm whereas the shunt resistance as an infinite. The working temperature is kept 300 K. The effect of absorption coefficient varying from $1 \cdot 10^4 \text{ cm}^{-1}$ to $1 \cdot 10^8 \text{ cm}^{-1}$ was simulated.

RESULTS AND DISCUSSIONS

Energy Band Diagram

Energy band diagram of proposed solar model “Glass/Back Contact/CZTS/ZnCdS/ZnO/Front Contact” is shown below and this is taken from the SCAPS-1D simulation software. The importance of this energy band diagram is to help out the discussion of optical properties of solar cell [35]. The band gap is adjusted by ZnCdS buffer layer in between CZTS absorber and ZnO window layers.

**Figure 3.** Energy band diagram

The visible light is absorbed throughout the absorber as well as at the heterojunction. The bandgap value for incident light photons that is ideal for most of the light to be absorbed for efficient power conversion efficiency is more or equal to 1.55 eV [36].

Effect of Zn Content

Under AM1.5 G 1 sun simulation was executed and at first we used ZnCdS buffer layer with 0% of Zn content and as a result Voc was 0.883483 V, Jsc was 22.55786 mA/cm², FF was 69.3755% and eta was 13.8262%. As the 1% of Zn content was dopped with CdS, its bandgap enhanced upto 2.58 eV, and at this bandgap Voc was 0.883434 V, Jsc was 22.54279 mA/cm², FF was 69.4027% and eta was recorded 13.8216%. All the parameters were decreased up to some extent because initially the Zn content was less in percentage and hence recombination of charges increased causing the decrement in the characteristics parameters of solar cell as shown in Table 4.

Table 4. Effect of Zn content on the characteristic's parameters of solar cell

Zn Content	ZnCdS band gap	Voc	Jsc	FF	Eta
%	eV	V	mA/cm ²	%	%
0	2.42	0.883483	22.55786	69.3755	13.8262
1	2.58	0.883434	22.54279	69.4027	13.8216
3	2.67	0.883421	22.5389	69.4176	13.822
5	2.78	0.883414	22.53656	69.4349	13.8239
10	2.90	0.883414	22.53607	69.4507	13.8267

But as the percentage of Zn content was gone on increasing the all characteristics parameters were also gone on increasing accordingly. The effect is also shown in the following Figure 4. Finally, when Zn content of 10% doped, the Voc improved to 0.883414 V, Jsc increased up to 22.53607 mA/cm², FF reached 69.4507% and hence the efficiency achieved 13.8267%. This value of efficiency is more than the efficiency at pure CdS. Finally, it is proved that as the Zn content increased the efficiency was also increased to some extent.

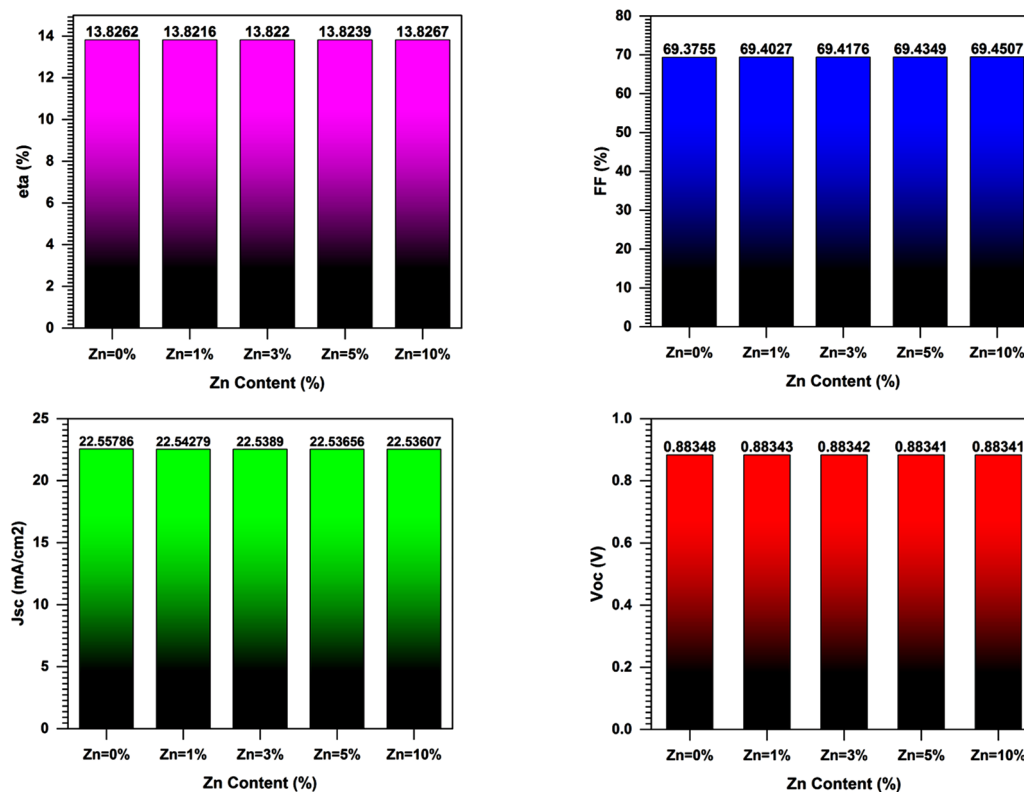


Figure 4. Effect of Zn content on Characteristics parameters of solar cell

The pattern of Zn content on the performance of solar cell is also shown on the J-V characteristic curve of solar device in following Figure 5. Effect of Zn content on J-V curve is same as in efficiency of cell as discussed above. Initially when there is 0% content of Zn and bandgap is 2.42 eV, its curve shows gud performance than 1%, 3% and 5% content of Zn with ZnCdS having 2.58 eV, 2.67 eV and 2.78 eV of bandgap respectively.

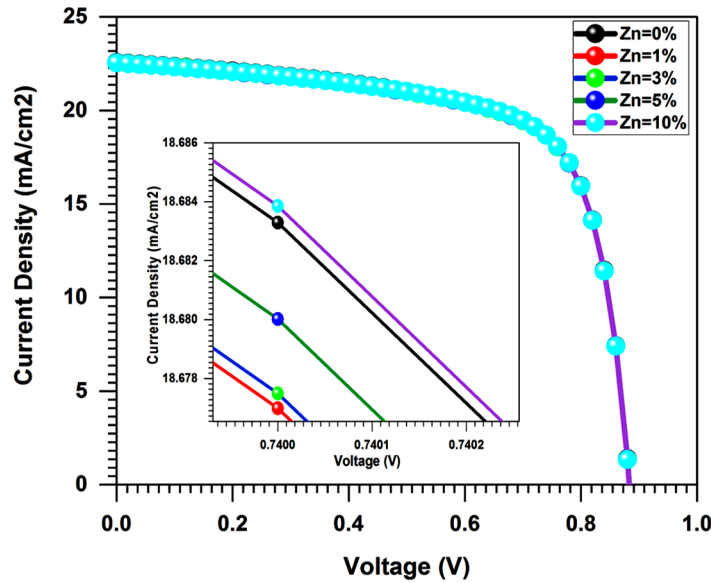


Figure 5. Effect of Zn content on J-V curve of the proposed solar cell

But at 10% content of Zn giving the 2.90 eV gave the most improved curve with skyblue bubbles as shown in Figure 5.

Effect of CZTS Thickness

Because the optimum Zn concentration value of 10% produced satisfactory results, ZnCdS with a bandgap of 2.90 was simulated using a buffer layer of 0.1 μm thickness.

Table 5. CZTS Thickness effect on Characteristics Parameters

CZTS Thickness	Voc	Jsc	FF	eta
um	V	mA/cm ²	%	%
1.5	0.88339	22.52569	69.457	13.82123
2.0	0.88342	22.53815	69.45105	13.82813
2.5	0.88341	22.5484	69.4465	13.83345
3.0	0.88345	22.5571	69.44461	13.83897
3.5	0.88344	22.56487	69.4324	13.84117

As a window layer, ZnO with a thickness of 0.05 μm was used. Working temperature was held at 300K under A.M 1.5 G 1 solar irradiation, and simulation was performed by changing thickness of the CZTS absorber layer from 1.5 to 3.5 μm.

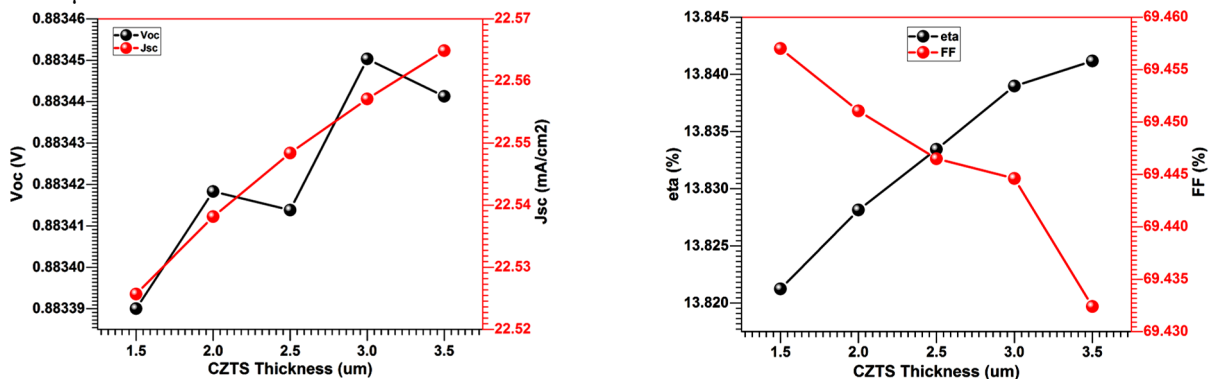


Figure 6. Effect of CZTS layer thickness on Characteristics parameters curves

Voc was 0.88339 V at 1.5 μm, Jsc was 22.525 mA/cm², FF was 69.457 %, and eta was 13.821 %. The open circuit voltages climbed to 0.88342 V as the thickness grew from 1.5 to 2.0 μm, and the current density increased to 22.538 mA/cm², while the factor fell to 69.451 %, yet efficiency improved to 13.828 %. The thickness of CZTS was then adjusted to 2.5 μm, and the Voc, Jsc, FF, and eta were reported as 0.88341 V, 22.548 mA/cm², 69.446 %, and 13.833%, respectively, at this thickness. Finally, when the thickness was raised from 3.0 to 3.5 μm, Voc went from 0.88345 to 0.88344 V, and Jsc went from 22.5571 to 22.5648 mA/cm². Similarly, FF varied from 69.4446 to 69.4324 %, while eta varied from 13.8389 to 13.8411 % as shown in Table 5 and Figure 6.

Temperature Effect

From the above results and discussion, we conclude the optimized Zn content of 10% with bandgap 2.90 eV of ZnCdS along with the CZTS optimum layer thickness of 3.5 μm , the simulation was run again to check an effect of working temperature on performance of solar device.

The temperature was varied from 280 to 350 K. At 280 K temperature, V_{oc} was 0.9535 V, J_{sc} 22.6074 mA/cm^2 , FF 70.208% and efficiency raised to 14.846%. As the temperature is very low hence the heating effect on the solar cell is negligible that's why its efficiency raised to 14.846%. This is very fruitful improvement because of temperature.

But as temperature rises from 280 to 350 K, all the parameters are affected largely as shown in Table 6 and Figure 7.

Table 6. Temperature effect on Characteristics Parameters

Temperature	V_{oc}	J_{sc}	FF	eta
K	V	mA/cm^2	%	%
280	0.93535	22.60743	70.20864	14.84627
290	0.9094	22.58729	69.84021	14.34577
300	0.88344	22.56487	69.43240	13.84117
310	0.85725	22.54034	68.99134	13.33098
320	0.83086	22.51415	68.50709	12.81500
330	0.80449	22.48712	67.97279	12.29675
340	0.77797	22.46051	67.39014	11.77553
350	0.75123	22.43615	66.75632	11.25160

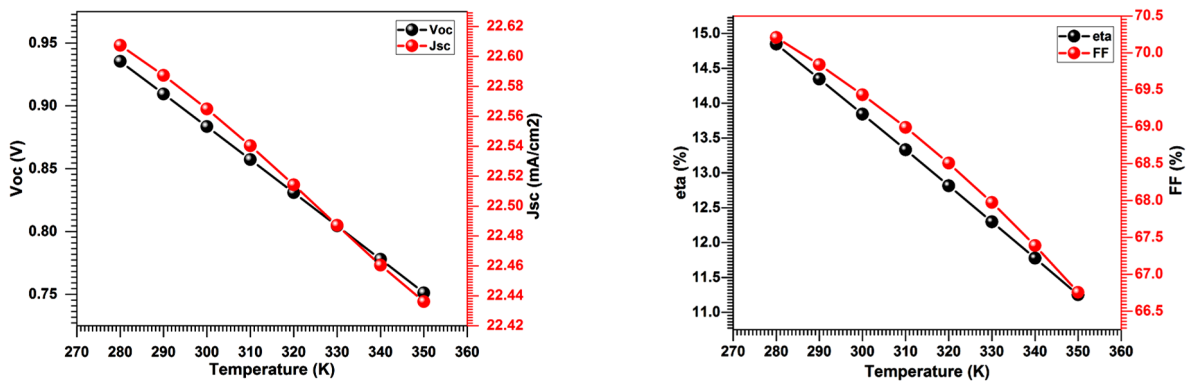


Figure 7. Temperature effect on Characteristics parameter curves

At 290 K of temperature the V_{oc} decreased to 0.9094 V, J_{sc} also decreased to 22.5872 mA/cm^2 , FF 69.84% and efficiency decreased up to 14.34% from 14.846%. Because as the temperature rises, the collision of electrons and holes increases and due to their collision, the flow of these charges slow down hence causing the less generation of potential as a result efficiency decreases. The negative effect of increasing temperature is also shown in J-V curve as shown in the Figure 8.

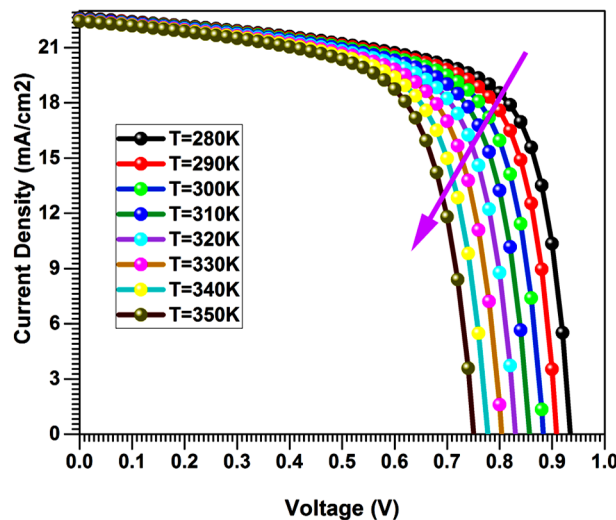


Figure 8. Temperature effect on J-V curve

A negative effect of rising temperature is not only on the characteristic's parameters (V_{oc} , J_{sc} , FF and η) and not on J-V curve, but it imparts its effect on the quantum efficiency. As quantum efficiency is a ratio of carriers collected by the solar cell to number of photons of sunlight incident on the solar cell. So as by increasing the temperature, its curve is moving down, that means the ratio is decreasing which ensures that number of carriers collecting on solar device surface are decreasing because of increasing temperature as shown in Figure 9.

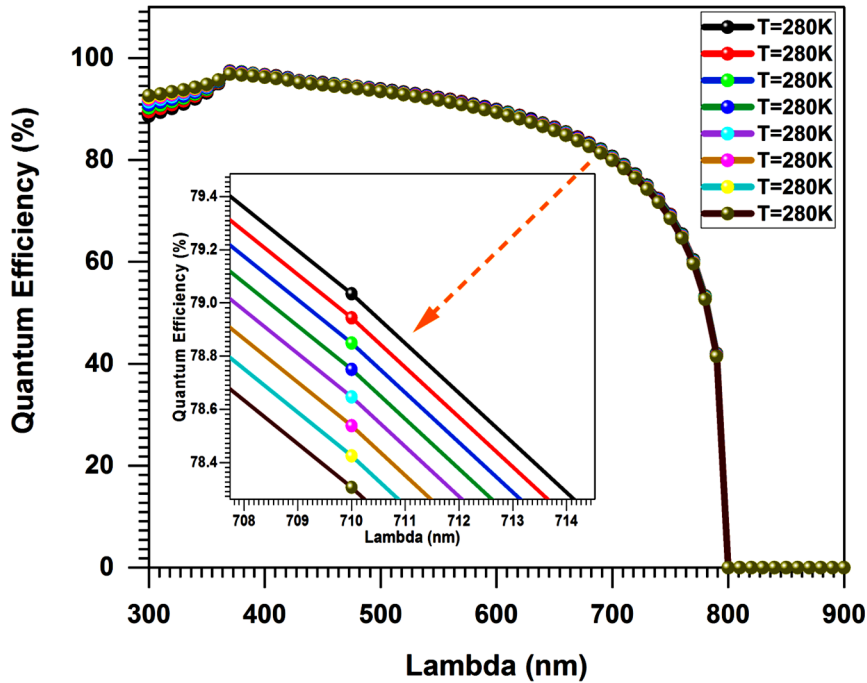


Figure 9. Temperature effect on Quantum Efficiency of Solar Cell

Finally at 350K, V_{oc} changed from 0.93535 to 0.75123 V, J_{sc} decreased from 22.60743 to 22.43615 mA/cm², FF from 70.20864 to 66.75632% and η effect the most from 14.84627 to 11.2516%.

Effect of Absorption Coefficient

Proposed solar cell “Back Contact/Glass/CZTS/ZnCdS/ZnO/Front Contact” was simulated at 300 K temperature under AM 1.5 G 1 SUN. The optimized thickness of CZTS of 3.5 μm , Zn contented ZnCdS having optimized bandgap of 2.90 with 0.1 μm thickness and ZnO with fixed thickness of 0.05 μm were used in the simulation program. The penetration of sun light in the solar cell has the major role on its efficiency. Because as much light will penetrate in the solar cell material, the more light will be able to absorbed. So, absorption coefficient tells about this absorption. As the absorption coefficient increases, the number of photons going to be absorbed is also increased. Hence to check an effect of absorption coefficient on a performance of solar device, its value was varied from $1 \cdot 10^4$ to $1 \cdot 10^9 \text{ cm}^{-1}$.

At $1 \cdot 10^4 \text{ cm}^{-1}$ of absorption coefficient, the V_{oc} was 0.8158 V, J_{sc} 6.447 mA/cm², FF was 60.635% and η was only 3.189%. But as the absorption coefficient was increased the characteristics parameters were also increased as shown in Table 7. At $1 \cdot 10^5 \text{ cm}^{-1}$ absorption coefficient, V_{oc} was increase upto 0.882 V. But in J_{sc} there was very surprisingly increment was observed from 6.44 to 22.10 mA/cm² with FF 68.89%. There was a remarkable effect of absorption coefficient on the efficiency of solar cell because it was improved from 3.18% to 13.43%. This effect can be observed in the Figure 10 of characteristics parameters of solar cells also. The absorption coefficient was varied upto $1 \cdot 10^9 \text{ cm}^{-1}$ and at this value the V_{oc} was recorded 0.8917 V, J_{sc} of 25.92%, FF upto 70.278% and efficiency boost up to 16.24%.

Table 7. Absorption Coefficient Effect on Characteristics Parameters

Absorption Coefficient	V_{oc}	J_{sc}	FF	η
cm^{-1}	V	mA/cm^2	%	%
1.00×10^4	0.81587	6.447810	60.63543	3.189760
1.00×10^5	0.88202	22.10740	68.89824	13.43457
1.00×10^6	0.89316	26.09574	71.73494	16.71967
1.00×10^7	0.89199	26.02355	70.33203	16.32608
1.00×10^8	0.89168	25.87128	70.30721	16.21917
1.00×10^9	0.89170	25.92108	70.27816	16.24390

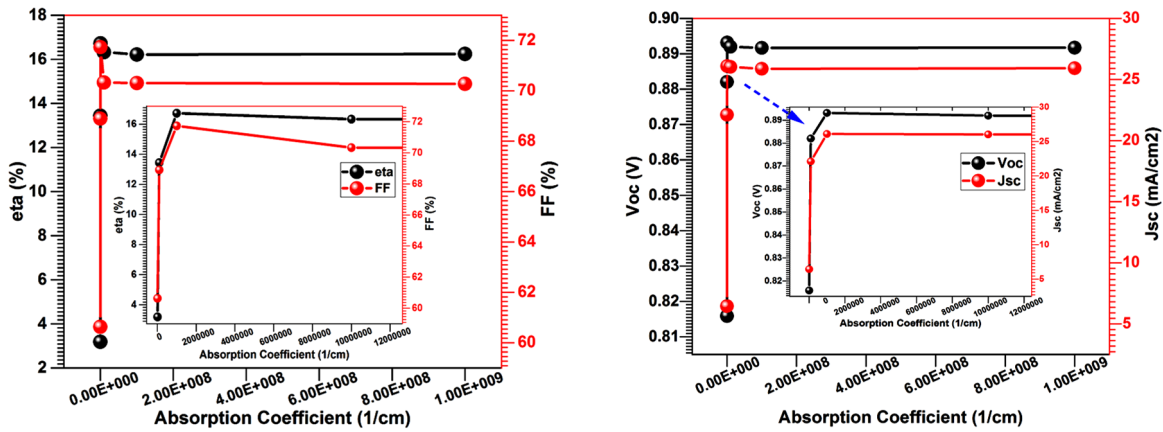


Figure 10. Effect of Absorption coefficient on characteristic parameters curves

Figure 11 represents the effect of absorption coefficient on J-V characteristic curve of solar cell. From the curve it is investigated that by increasing an absorption coefficient, the curve goes up going away from the origin showing the improvement in the performance of solar cell.

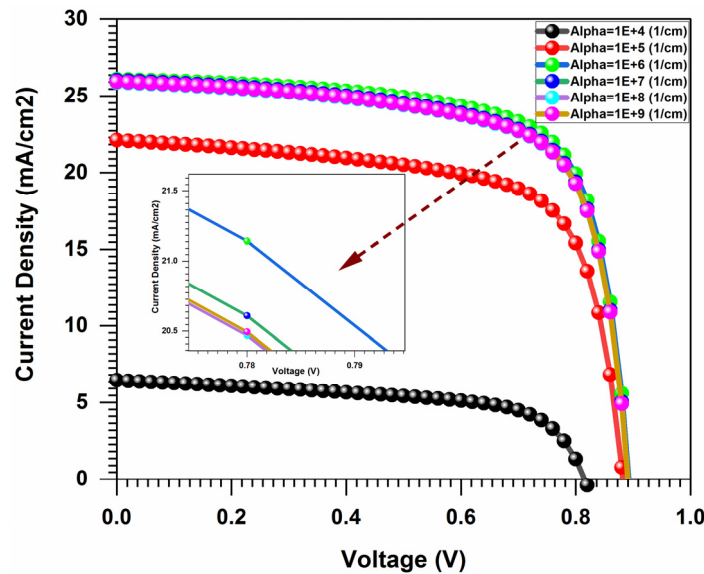


Figure 11. Effect of Absorption coefficient on characteristic parameters curves

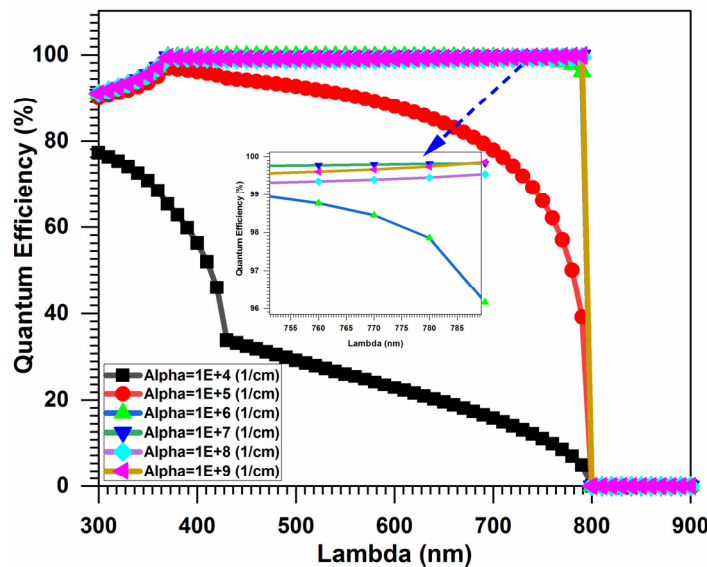


Figure 12. Effect of Absorption coefficient on Quantum Efficiency of solar cell.

Quantum efficiency graph in Figure 12 shows the effect of absorption coefficient. As the absorption coefficient increases, the graph improves to upward matching to 100% quantum efficiency showing an enhancement in the performance of solar cell.

CONCLUSION





Proposed solar cell model “*Back Contact/CZTS/ZnCdS/ZnO/Front Contact*” was simulated to investigate an effect of ZnCdS buffer layer varied bandgap on the performance of solar cell. By increasing the bandgap of ZnCdS the performance of solar is improved hence the role of Zn content in ZnCdS has definite impact because all characteristics parameters were changed at different content of Zn. At 10% Zn content ZnCdS has 2.90 eV, and this was the optimized value at which we got maximum efficiency of 13.826% along with 69.45% fill factor. Later on the effect of CZTS absorber layer was observed on characteristics parameters and J-V curve of the solar cell. Thickness of CZTS was varied from 1.5 μm to 3.5 μm . The optimized thickness was 3.5 μm because at this thickness efficiency was 13.841% which was initially 13.826%. After optimization of Zn content and CZTS absorber layer, the effect of working temperature was observed by varying it from 280 K to 350 K. By increasing temperature the efficiency decreased from 14.84% to 11.25% for 280K to 350K. But it is note able that as the temperature was decreased from 300K (normal temperature) to 280K, the efficiency was increased from 13.82% to 14.84%. At the end the effect of absorption coefficient was studied by varying it from $1 \cdot 10^4$ to $1 \cdot 10^9$. At $1 \cdot 10^9$, the efficiency boost up to 16.24%. After optimization of all parameters, simulation was run at 280K, having CZTS thickness of 3.5 μm , with 10% content Zn in ZnCdS (2.90 eV), and absorption coefficient of $1 \cdot 10^9$, the model efficiency reached up to 17.6% with Voc of 0.994 V, Jsc 26.1 mA/cm² and Fill factor was 71.4%. These results are very remarkable and will be very useful for the researcher’s consideration during synthesis of this “*Back Contact/CZTS/ZnCdS/ZnO/Front Contact*” purposed model type solar cell and the simulation results may be utilized experimentally to build “CZTS/ ZnCdS /ZnO” based solar cells in future with optimization of this work.

Acknowledgement

This work was supported by European commission under project Erasmus+ (2019-1-ES01-KA107-062073), Coordinator University Polytechnic of Valencia, Spain and Grant PID2019-107137RB-C22 funded by MCIN/AEI/10.13039/501100011033 and by “ERDF A way of making Europe. Authors also acknowledged Dr. Marc Burgelman for providing the software SCAPS-1D.

Conflict of Interest. Authors declared that there is no conflict of interest.

ORCID IDs

 **Muhammad Aamir Shafi**, <https://orcid.org/0000-0001-9813-7029>;
  **Hanif Ullah**, <https://orcid.org/0000-0002-0529-973X>
 **Laiq Khan**, <https://orcid.org/0000-0003-3659-3824>;
  **Bernabe Mari**, <https://orcid.org/0000-0003-0001-419X>

REFERENCES

- [1] Repins, S. Glynn, J. Duenow, T.J. Coutts, W.K. Metzger, and M.A. Contreras, in: *Proc. SPIE 7409, Thin Film Solar Technology*, 74090M (United States, 2009), <https://doi.org/10.1117/12.828365>
- [2] H. Khallaf, I.O. Oladeji, G. Chai, and L. Chow, “Characterization of CdS thin films grown by chemical bath deposition using four different cadmium sources”, *Thin Solid Films*. **516**(21), 7306 (2008), <https://doi.org/10.1016/j.tsf.2008.01.004>
- [3] L.S.S. Singh, K.P. Tiwary, R.K. Purohit, Z.H. Zaidi, and M. Husain, “ECR plasma etching of GaAs in CCl₂F₂/Ar/O₂ discharge and IR studies of the etched surface”, *Current Applied Physics*, **5**(4), 351 (2005), <https://doi.org/10.1016/j.cap.2004.04.002>
- [4] S.K. Choubey, A. Kaushik, and K.P. Tiwary, “Structural and optical properties of pure and Mg doped CdSe nanoparticles synthesized by microwave assisted method”, *Chalcogenide Letters*, **15**(3), 125 (2018), https://chalcogen.ro/125_ChoubeyS.pdf
- [5] R. Kumar, R. Praveen, S. Rani, K. Sharma, K.P. Tiwary, and K.D. Kumar, “ZnSe Nanoparticles Reinforced Biopolymeric Soy Protein Isolate Film”, *Journal of Renewable Materials*, **7**(8), 749 (2019), <https://www.techscience.com/jrm/v7n8/30575>
- [6] S.K. Choubey, and K.P. Tiwary, *Digest Journal of nanomaterials and Biostructures*, **11**(1), 33 (2016), https://chalcogen.ro/33_Choubey.pdf
- [7] S.K. Choubey, and K.P. Tiwary, *International Journal of Innovative Research in Science, Engineering and Technology*, **3**(3), 10670 (2014), <https://techjournals.stmjournals.in/index.php/NTs/article/download/829/747>
- [8] B.S. Tosun, C. Pettit, S.A. Campbell, and E.S. Aydil “Structure and Composition of ZnxCd1-xS Films Synthesized through Chemical Bath Deposition”, *ACS Appl. Mater. Interfaces*. **4**(7), 3676 (2012), <https://doi.org/10.1021/am300771k>
- [9] J. Song, S.S. Li, S. Yoon, J. Song., S.S. Li, S. Yoon, W.K. Kim, J. Kim, J. Chen, V. Craciun, T.J. Anderson, O. D. Crisalle, and F. Ren, “Growth and characterization of CdZnS thin film buffer layers by chemical bath deposition”, in: *Conference Record of the IEEE Photovoltaic Specialists Conference*, (IEEE, 2005), pp. 449-452.
- [10] S. Kumar, and K.P. Tiwary, “ZnCdS thin film chalcogenide by chemical bath deposition method”, *Nanotrends AJ Nanotechnol Appl.*, **22**(1), 19 (2020), <https://techjournals.stmjournals.in/index.php/NTs/article/download/829/747>
- [11] T.P. Kumar, S. Saravanakumar, and K. Sankaranarayanan, “Effect of annealing on the surface and band gap alignment of CdZnS thin films”, *Applied Surface Science*, **257**(6), 1923-1927 (2011), <http://dx.doi.org/10.1016%2Fj.apsusc.2010.09.027>
- [12] C. Xing, Y. Zhang, W. Yan, and L. Guo, “Band structure-controlled solid solution of Cd1-x Zn_xS photocatalyst for hydrogen production by water splitting”, *International Journal of Hydrogen Energy*, **31**(14), 2018 (2006), <https://doi.org/10.1016/j.ijhydene.2006.02.003>
- [13] S. Horoz, Q. Dai, F. S. Maloney, B. Yakami, J. M. Pikal, X. Zhang, J. Wang, W. Wang, and J. Tang, “Absorption induced by Mn doping of ZnS for improved sensitized quantum-dot solar cells”, *Physical Review Applied*, **3**(2), 024011 (2015), <https://doi.org/10.1103/PhysRevApplied.3.024011>

- [14] P.K. Santra, and P.V. Kamat, "Mn-doped quantum dot sensitized solar cells: a strategy to boost efficiency over 5%", Journal of the American Chemical Society, **134**(5), 2508 (2012), <https://doi.org/10.1021/ja211224s>
- [15] J.K. Salem, T.M. Hammad, S. Kuhn, M.A. Draaz, N.K. Hejazy, R. Hempelmann, J. Mater. Sci: Mater. Electron, **25**, 2177 (2014), <https://doi.org/10.1007/s10854-014-1856-8>
- [16] H.J. Liu, and Y.C. Zhu, "Synthesis and characterization of ternary chalcogenide ZnCdS 1D nanostructures", Materials Letters, **62**(2), 255 (2008), <https://doi.org/10.1016/j.matlet.2007.05.011>
- [17] B. Kumar, P. Vasekar, S.A. Pethe, N.G. Dhere, and G.T. Koishiyev, Thin Solid Films, **517**, 2295 (2009), <https://doi.org/10.1016/j.tsf.2008.10.108>
- [18] B. Dawoud, E.H. Amer, and D.M. Gross, "Experimental investigation of an adsorptive thermal energy storage", International journal of energy research, **31**(2), 135 (2007), <https://doi.org/10.1002/er.1235>
- [19] M.C. Baykul, and N. Orhan, "Band alignment of Cd (1-x) Zn_xS produced by spray pyrolysis method", Thin Solid Films, **518**(8), 1925 (2010), <https://doi.org/10.1016/j.tsf.2009.07.142>
- [20] A.J. Clayton, M.A. Baker, S. Babar, R. Grilli, P.N. Gibson, G. Kartopu, D.A. Lamb, V. Barrioz, and S.J.C.Irvine, "Effects of Cd_{1-x}Zn_xS alloy composition and post-deposition air anneal on ultra-thin CdTe solar cells produced by MOCVD", Materials Chemistry and Physics, **192**, 244 (2017), <https://doi.org/10.1016/j.matchemphys.2017.01.067>
- [21] I. Levchuk, C. Würth, F. Krause, A. Osvet, M. Batentschuk, U.R. Genger, C. Kolbeck, P. Herre, H.P. Steinrück, W. Peukert, and C.J. Brabec, Energy Environ. Sci. **9**, 1083 (2016), <https://doi.org/10.1039/C5EE03165F>
- [22] B. Kumar, P. Vasekar, S.A. Pethe, N.G. Dhere, and G.T. Koishiyev, "ZnxCd1-xS as a heterojunction partner for CuIn1-xGaxS2 thin film solar cells", Thin Solid Films, **517**(7), 2295 (2009), <https://doi.org/10.1016/j.tsf.2008.10.108>
- [23] B. Bibi, B. Farhadi, N. Rahman, and A. Liu, "A novel design of CZTS/Si tandem solar cell: A numerical approach", (2021), <https://doi.org/10.21203/rs.3.rs-309446/v1>
- [24] M.A. Shafi, A. Bouich, K. Fradi, J.M. Guaita, L. Khan, and B. Mari, "Effect of Deposition Cycles on the Properties of ZnO Thin Films Deposited by Spin Coating Method for CZTS-based Solar Cells", Optik, 168854 (2022), <https://doi.org/10.1016/j.ijleo.2022.168854>
- [25] M.A. Shafi, L. Khan, S. Ullah, A. Bouich, H. Ullah, and B. Mari, "Synthesis of CZTS kesterite by pH adjustment in order to improve the performance of CZTS thin film for photovoltaic applications", Superlattices and Microstructures, 107185 (2022), <https://doi.org/10.1016/j.spmi.2022.107185>
- [26] S. Chen, J.H. Yang, X.G. Gong, A. Walsh, and S.H. Wei, "Intrinsic point defects and complexes in the quaternary kesterite semiconductor Cu₂ZnSnS₄", Physical Review B, **81**(24), 245204 (2010), <https://doi.org/10.1103/PhysRevB.81.245204>
- [27] A. Cherouana, and R. Labbani, "Numerical simulation of CZTS solar cell with silicon back surface field", Materials Today: Proceedings, **5**(5), 13795 (2018), <https://doi.org/10.1016/j.matpr.2018.02.020>
- [28] M.A. Shafi, L. Khan, S. Ullah, M.Y. Shafi, A. Bouich, H. Ullah, and B. Mari, "Novel Compositional Engineering for ~ 26% Efficient CZTS-Perovskite Tandem Solar Cell", Optik, **253**, 168568 (2022), <https://doi.org/10.1016/j.ijleo.2022.168568>
- [29] H. Movla, D. Salami, and S.V. Sadreddini, "Simulation analysis of the effects of defect density on the performance of pin InGa_N solar cell", Applied Physics A, **109**(2), 497 (2012), <https://doi.org/10.1007/s00339-012-7062-8>
- [30] R.S. Crandall, "Modeling of thin film solar cells: Uniform field approximation", Journal of Applied Physics, **54**(12), 7176 (1983), <https://doi.org/10.1063/1.331955>
- [31] M. Uddin, M.S. Hossain, and N. Amin, Study on the prospects of Sb₂Te₃ back surface field in ZnCdS/ZnCdTe thin film solar cell, in: *2015 2nd International Conference on Electrical Information and Communication Technologies (EICT)*, (IEEE, 2015), pp. 403-406.
- [32] S.K. Pandey, and K. Kumar, "Device Modelling and Performance Analysis of CZTS/CdTe Solar Cell", Advanced Science, Engineering and Medicine, **11**(5), 351 (2019), <https://doi.org/10.1166/aseem.2019.2362>
- [33] S. Ullah, H. Ullah, F. Bouhjar, M. Mollar, B. Mari, and A. Chahboun, "Influence of zinc content in ternary ZnCdS films deposited by chemical bath deposition for photovoltaic applications", ECS Journal of Solid State Science and Technology, **7**(8), P345 (2018), <https://doi.org/10.1149/2.0021808jss>
- [34] M.A. Shafi, H. Ullah, S. Ullah, L. Khan, S. Bibi, and B.M. Soucase, "Numerical Simulation of Lead-Free Sn-Based Perovskite Solar Cell by Using SCAPS-1D", Engineering Proceedings, **12**(1), 92 (2022), <https://doi.org/10.3390/engproc2021012092>
- [35] Y. Hamakawa, H. Okamoto, and Y. Nitta, "A new type of amorphous silicon photovoltaic cell generating more than 2.0 V", Applied Physics Letters, **35**(2), 187 (1979), <https://doi.org/10.1063/1.91031>
- [36] M.M.A. Moon, M.H. Ali, M.F. Rahman, J. Hossain, and A.B.M. Ismail, "Design and Simulation of FeSi₂-Based Novel Heterojunction Solar Cells for Harnessing Visible and Near-Infrared Light", Physica Status Solidi (a), **217**(6), 1900921 (2020), <https://doi.org/10.1002/pssa.201900921>

ЧИСЛОВЕ МОДЕЛЮВАННЯ ДЛЯ ПІДВИЩЕННЯ ЕФЕКТИВНОСТІ ТОНКОПЛІВКОВОГО СОНЯЧНОГО ЕЛЕМЕНТУ НА ОСНОВІ CZTS З ВИКОРИСТАННЯМ SCAPS-1D

Мухаммад Аамір Шафіф^{a,e,f}, Сумайя Бібі^b, Мухаммад Муніб Хан^c,

Харун Сікандар^d, Фейсал Джавед^c, Ханіф Уллах^e, Лайк Хан^a, Бернабе Марі^f

^aФакультет електротехніки та комп'ютерної техніки, Університет COMSATS Ісламабад, Пакистан

^bФакультет електротехніки, Університет Бахауддіна Закарії, Мултан, Пакистан

^cФакультет електротехніки, Пакистан Інститут Південного Пенджабу Мултан, Пакистан

^dСЕМЕ, Коледж електротехніки та машинобудування, Нуст Ісламабад, Пакистан

^eФакультет електротехніки, Федеральний університет мистецтв і технологій урду, Ісламабад, Пакистан

^fІнститут дизайну та виробництва (IDF), Політехнічний університет Валенсії (UPV), Іспанія

У цій роботі ми запропонували сонячну батарею з моделлю «Задній контакт «Back Contact т/CZTS/ZnCdS/ZnO/Front Contact». CZTS працює як поглинаючий шар, ZnCdS як буферний шар і ZnO як віконний шар із заднім і переднім контактами. Вміст Zn змінювався від 0% до 10%, а заборонена зона змінювалася з 2,42 до 2,90 еВ, як описано в літературі. Вплив зміни ширини забороненої зони спостерігали на продуктивність сонячних елементів за допомогою програмного забезпечення SCAPS-1D.

Ефективність змінювалася за рахунок зміни ширини забороненої зони тонкоплівкового шару ZnCdS. Моделювання проводили при 300 К під час А.М. 1,5 Г 1 сонячного освітлення. Діаграма енергетичної забороненої зони була взята з SCAPS, щоб пояснити різні параметри сонячних елементів. Спостерігали вплив ZnCdS, що має різні значення ширини забороненої зони. Потім товщину шару CZTS змінювали, щоб перевірити його дію, і, отже, при 3,0 мкм забезпечили покращену ефективність у 13,83 %. Після оптимізації товщини шару CZTS було досліджено вплив робочої температури на продуктивність сонячного елемента. Зміна коефіцієнта поглинання від $1 \cdot 10^4$ до $1 \cdot 10^9 \text{ cm}^{-1}$ спричинила значний вплив на параметри характеристик сонячної батареї, а також на характеристики J-V і кривої квантової ефективності. При коефіцієнті поглинання $1 \cdot 10^9 \text{ cm}^{-1}$ ККД сонячних елементів збільшується до 16,24%. Це чудове підвищення ефективності сонячних елементів з 13,82% до 16,24%. Після оптимізації всіх параметрів моделювання проводилося при 280 К, товщина CZTS 3,5 мкм, з вмістом Zn в ZnCdS 10% (2,90 eV) і коефіцієнтом поглинання $1 \cdot 10^9$, ефективність моделі досягала 17,6% при Voc порядку 0,994 В, АТ 26,1 мА/см² і коефіцієнта заповнення 71,4%.

Ключові слова: ZnCdS; CZTS; моделювання; Ефективність; SCAPS-1D